Stabilizing Formation Systems With Nonholonomic Agents

Thomas L. Dearing, Xudong Chen, *Member, IEEE*, and Marco M. Nicotra, *Member, IEEE*

***Abstract*—This letter investigates the effects of adapting decentralized gradient-based control laws to nonholonomic agents in networked formation systems. Using the unicycle agent model and a standard cascade control structure, it is shown that the stability margins of the cascaded systems deteriorate as the numbers of agents increase. This trend indicates problems with both convergence and scalability. It is then shown that the asymptotic behaviors of the nominal gradient-based control laws can be recovered by introducing a bump function that allows forward motion only when the agents are oriented in appropriate directions. The proposed solution ensures almost global convergence and can be applied to formation systems of all sizes. Finally, comprehensive simulation results show that the usage of a bump function also reduces the total energy consumption required to reach a target formation.**

***Index Terms*—Cooperative control, nonholonomic systems, Lyapunov methods.**

I. Introduction

MULTI Agent Systems (MAS) have been gaining an increasing amount of traction over a wide range of applications where the coordination of multiple inexpensive systems is preferable to a complex centralized solution [1]. A primary factor to consider when designing a multi-agent control strategy is whether the agent dynamics are holonomic or nonholonomic. A system is called *holonomic* when it adheres to constraints of the form $f(q_1, \ldots, q_n, t) = 0$, i.e., its number of generalized coordinates q_i is equivalent to its controllable degrees of freedom [2]. Other constraints are called *nonholonomic* and introduce non-integrable path-dependencies to the system, allowing it to reach different configurations while achieving the same states q_i. For example, a wheel can be rotated by any angle by rolling it around and back in a closed path to the same position q_i.

In some cases, MAS's formally composed of nonholonomic agents are treated as holonomic under reasonable assumptions. Aircraft for example, can be approximated as holonomic systems during vertical take-off and landing under the assumption that the attitude dynamics are much faster than the position dynamics [3]. This has led to a variety of coordination strategies for aerial robotic swarms that assume holonomic behavior [4]. We direct the reader to [5] and the references therein for a survey of formation control that covers nonholonomic agents as special cases.

In this letter, we consider a new approach to the formation control of unicycle agents. This problem is not new, and many recent works on the subject (e.g., [6]–[8]) have presented exciting results in both flocking and tracking capabilities. However, these works require fixed target agent positions or displacements from a virtual center. In contrast, we consider the target *distances* between agents, a modification which (1) removes the need for a global coordinate system and (2) fundamentally changes the dynamics, associated stability issues, and the solutions addressing those issues. One work which has developed a distance-based control law is [9]. However, this law provides only local stability guarantees. In contrast, our result guarantees almost global convergence to the target formation if an appropriate graph is chosen.

This letter investigates how the reliance on time-scale separation can be problematic when a nominal multi-agent control strategy is adapted to a formation system with nonholonomic agents. By analyzing a MAS composed of unicycles, it is shown that certain gradient-based control laws become unstable in the presence of non-instantaneous attitude dynamics. Moreover, it is shown that this approach is not scalable as the time-scale separation needed to recover stability is a monotonically increasing function of the number of agents. To resolve this issue, we propose the use of bump functions as a means of adapting the nominal gradient-based control laws to nonholonomic (unicycle) agents. This solution is found to guarantee the same stability properties as the nominal gradient dynamics independent of the size of the MAS. It is also shown through extensive numerical simulations that the introduction of a bump function greatly improves control efficiency with respect to the unmodified coordination strategies.

Bump functions have been used extensively in the literature to smoothly stitch together potential functions, particularly when incorporating range-dependent behaviors such as collision avoidance [10]–[12]. To the author's best knowledge, the use of bump functions to bridge the gap between decentralized feedback control laws and nonholonomic agent dynamics is original to this letter. The main interest in this approach is

Manuscript received March 3, 2020; revised May 14, 2020; accepted June 8, 2020. Date of publication June 16, 2020; date of current version July 1, 2020. This work was supported in part by NSF under Grant ECCS-1809315. Recommended by Senior Editor S. Tarbouriech. *(Corresponding author: Thomas L. Dearing.)*

The authors are with the ECEE Department, University of Colorado Boulder, Boulder, CO 80528 USA (e-mail: thomas.dearing@colorado.edu; xudong.chen@colorado.edu; marco.nicotra@colorado.edu).

Digital Object Identifier 10.1109/LCSYS.2020.3002575

that it provides a simple, robust, and adaptable way to implement many existing networked control strategies such as [13] on nonholonomic agents.

This letter is organized as follows: Section II describes the intuitive approach used to implement holonomic coordination strategies on nonholonomic systems. Section III identifies the limitations of this approach and proposes a suitable modification that is guaranteed to ensure stability regardless of the number of agents. Section IV provides extensive simulation results which showcase the effectiveness and relative performance of the proposed solution. Finally, Section V summarizes this letter with concluding remarks.

II. Problem Formulation

A. Distance-Based Formation Control

In this letter, we address the control problem of stabilizing n mobile, autonomous agents to prescribed distances from each other. The information flow topology of a formation system is represented by a connected, undirected graph $G = (\mathcal{V}, \mathcal{E})$ where $\mathcal{V}$ is the set of nodes (agents), $\mathcal{E}$ is the set of edges, and $(i, j) \in \mathcal{E}$ indicates that agents i and j can communicate with each other. Given the position $z_i = [x_i, y_i]^\top \in \mathbb{R}^2$, let $d_{ij}(t) := \|z_j(t) - z_i(t)\|_2$ be the distance between agents i and j at time t. Then, a formation $(z_1, \ldots, z_n)$ is said to be a *target formation* if the relative distances d_{ij} match certain desired inter-agent distances $\bar{d}_{ij} \in \mathbb{R}_{>0}$ for each $(i, j) \in \mathcal{E}$. If G is infinitesimally rigid, there are only finitely many target formations (modulo rotations and translations). We say that a formation system has reached a target formation when $\|z_i(t) - z_j(t)\| = \bar{d}_{ij}$ for all $(i, j) \in \mathcal{E}$. For bearing and angle-based formation control, the reader is referred to [14], [15] and references therein.

Given a networked system of n agents subject to the simplified dynamic model

$$\dot{x}_i(t) = u_{x,i}(t), \quad \dot{y}_i(t) = u_{y,i}(t), \tag{1}$$

consider the following *nominal* feedback law based on earlier works [16]–[18],

$$\begin{bmatrix} u_{x,i} \\ u_{y,i} \end{bmatrix} := \boldsymbol{F}_i = k_v \sum_{j \in \mathcal{N}_i} a(d_{ij}, \bar{d}_{ij})(\boldsymbol{z}_j - \boldsymbol{z}_i), \tag{2}$$

where $k_v \in \mathbb{R}_{\geq 0}$ is the unicycle's forward velocity control gain, $\mathcal{N}_i = \{j \mid (j, i) \in \mathcal{E}\}$ is the set of neighbors for agent i, and the *interaction law* $a(\cdot, \bar{d}_{ij}) : \mathbb{R}_{\geq 0} \to \mathbb{R}$ is a strictly increasing C^1-function for each fixed $\bar{d}_{ij}$, and satisfies $a(\bar{d}_{ij}, \bar{d}_{ij}) = 0$. In future, we use the notation $a_{ij}(s) := a(s, \bar{d}_{ij})$ for each edge $(i, j) \in \mathcal{E}$. As detailed in [18], the controlled system (1)-(2) follows the gradient descent of the potential function

$$\Phi(\boldsymbol{z}) = k_v \sum_{(j,i) \in \mathcal{E}} \int_{\bar{d}_{ij}}^{d_{ij}} a_{ij}(|s|) s ds, \quad \frac{\partial \Phi}{\partial z_i} = -\boldsymbol{F}_i. \tag{3}$$

As with any multi-agent gradient-descent formulation, (3) is guaranteed to converge to a local minimum from *almost* all Initial Conditions (ICs).

To express this precisely, we let $\mathcal{A} := \{z \mid \partial \Phi / \partial z = 0\}$ be the set of *critical formations* of Φ (that is, both stable and unstable equilibria). If the potential function Φ is an equivariant Morse function with respect to the group SE(2) of rigid motions [19], [20], then the set $\mathcal{A}$ is finite modulo rotations and translations. For example, this is the case when the underlying graph G is a triangulated Laman graph and some other mild assumptions on a are satisfied (see [18]). Let $\mathcal{A}_1 \subseteq \mathcal{A}$ be the set of local minima of Φ (stable equilibria). Then, the stable manifolds of $\mathcal{A}_1$ are open and dense in the entire state space of the formation system. As such, we say that the dynamics (2) are *almost globally convergent* to formations in $\mathcal{A}_1$ or equivelantly that $\mathcal{A}_1$ is *almost globally stable*. Moreover, if G is a triangulated Laman graph, then it is shown in [18] that $\mathcal{A}_1$ contains only desired target formations, and (2) renders $\mathcal{A}_1$ almost globally asymptotically stable. For issues concerning the strict global stability of such systems, we refer the reader to [21].

B. Formation Control With Unicycles

In many applications, the individual agent dynamics are nonholonomic. For example, consider the unicycle dynamics

$$\begin{aligned} \dot{x}_i &= u_{v,i} \cos\theta_i, \\ \dot{y}_i &= u_{v,i} \sin\theta_i, \\ \dot{\theta}_i &= u_{\tau,i}, \end{aligned} \tag{4}$$

where $\theta_i \in \mathbb{R}$ is the angle between the x-axis and the agent's forward direction, and $u_{v,i}$, $u_{\tau,i}$ are the control inputs for forward movement and rotation. These dynamics are nonholonomic due to the zero lateral velocity constraint

$$\dot{x}_i \sin(\theta_i) - \dot{y}_i \cos(\theta_i) = 0.$$

For convenience, the agent's position and orientation vectors are concatenated as $\boldsymbol{z} := [\boldsymbol{z}_1; \cdots; \boldsymbol{z}_n]$ and $\boldsymbol{\theta} := [\theta_1; \cdots; \theta_n]$. Note that results obtained using this simple kinematic model can be adapted to force-controlled models using appropriate velocity-tracking controllers (see [6]).

For this model to converge to a target formation under the same information flow assumptions as (1), an intuitive approach is to adapt the nominal feedback law (2) to the unicycle dynamics (4). Specifically, given the real-time target orientation resulting from the nominal feedback control law $\bar{\theta}_i = \text{atan2}(\boldsymbol{F}_i)$, consider the inner-outer loop controller

$$u_{v,i} = \|\boldsymbol{F}_i\|_2, \qquad u_{\tau,i} = -k_\theta \tilde{\theta}_i, \tag{5}$$

where $k_\theta \in \mathbb{R}_{\geq 0}$ is the orientation control gain, and $\tilde{\theta}_i := ((\theta_i - \bar{\theta}_i) + \pi \mod 2\pi) - \pi$ is the agent's orientation error (shown in Figure 1) rounded to $(-\pi, \pi]$ via the modulus function. Note that this definition of $\tilde{\theta}_i$ can switch rapidly at the $\pm\pi$ boundary, but this can be corrected by the hysteresis extension $\tilde{\theta}_i \in (-(\pi + \epsilon), \pi + \epsilon)$ for some $\epsilon > 0$.

As is shown in Figure 2, the position dynamics $\dot{\boldsymbol{z}}$ are driven by the outer-loop, which are based on the nominal control law (2), whereas the orientation dynamics $\dot{\boldsymbol{\theta}}$ are controlled separately via an inner-loop feedback. Combining (4) and (5), the closed loop dynamics are

$$\begin{aligned} \dot{\boldsymbol{z}}_i &= \boldsymbol{R}(\tilde{\theta}_i)\boldsymbol{F}_i, \\ \dot{\theta}_i &= -k_\theta \tilde{\theta}_i, \qquad \boldsymbol{R}(\tilde{\theta}_i) = \begin{bmatrix} \cos\tilde{\theta}_i & -\sin\tilde{\theta}_i \\ \sin\tilde{\theta}_i & \cos\tilde{\theta}_i \end{bmatrix}, \end{aligned} \tag{6}$$

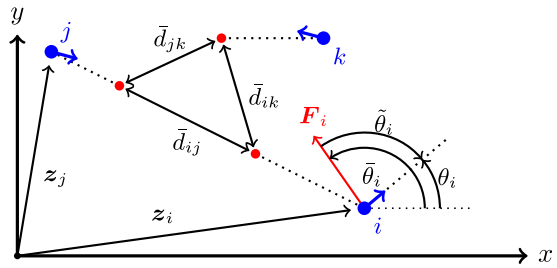

Fig. 1. Unicycle Formations in $\mathbb{R}^2$. The current physical positions and orientations of the agents are indicated in blue, while a target formation and the nominal gradient-descent direction $\boldsymbol{F}_i$ from (2) are shown in red.

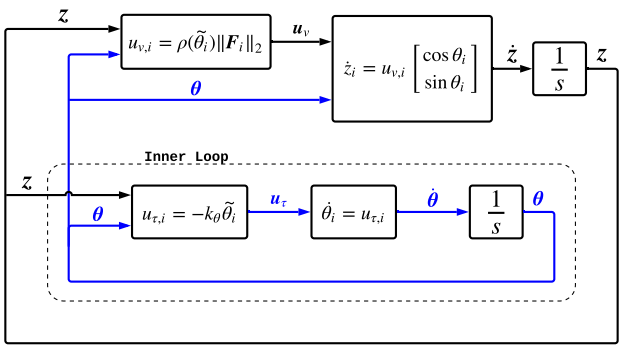

Fig. 2. Unicycle Cascade Feedback Diagram.

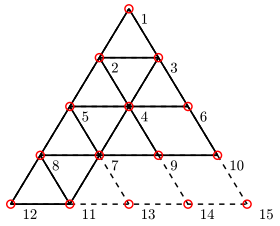

Fig. 3. Rigid Laman graphs by iterative Henneberg construction. This construction is used for simulations in both unbounded and bounded cases.

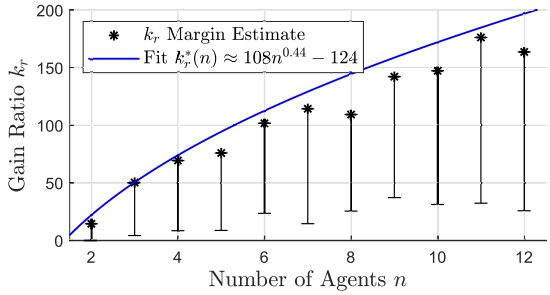

Fig. 4. Numerical approximation of the stability boundary $k_r^*(n)$ for the unbounded interaction law $a = d_{ij} - \bar{d}_{ij}$. $k_r^*(n)$ was estimated for each n using bisection for 100 random deployments. A least-square fit of the pointwise maximum of these results is also provided.

where the rotation matrix $R(\tilde{\theta}_i)$ captures the misalignment of the unicycle's orientation from (2).

To ensure stability, this approach fundamentally assumes that the inner-loop (orientation) dynamics are much faster than the outer loop (position) dynamics [22]. This requirement is captured by the gain ratio $k_r := k_\theta/k_v$. One would expect that, as $k_r \to \infty$, the behavior of the new system (6) will be comparable to the nominal system (2). As is detailed in the next section however, this is not sufficient to ensure stability for an arbitrary number of agents.

III. Stability Issues and a Scalable Solution

In this section, we examine the stability of (6) in the presence of unbounded and bounded interaction laws. We then present a slight modification which guarantees almost global convergence to the target formation.

A. Unbounded Interaction Laws

Consider the case where the interaction law $a_{ij}(s)$ is unbounded so that $\|a_{ij}\|_\infty = \infty$ and $\|F_i\|$ is not globally Lipschitz. Intuitively, the stability of (6) is dependent on the gain ratio $k_r := k_\theta/k_v$. Indeed, if the orientation errors are sufficiently large (i.e., $|\tilde{\theta}_i| > \pi/2$), the agents will initially move *away* from their target positions. Given a sufficiently large initial separation, the agents are then at risk of accelerating in an outward spiral if k_r is not large enough to quickly re-orient them inwards. The simulations in Figure 4 support this hypothesis for the unbounded interaction law $a_{ij}(d_{ij}) = d_{ij} - \bar{d}_{ij}$. The results were obtained by constructing Laman graphs of size $n = 2$ to $n = 12$ using the method illustrated in Figure 3. Given the target distances $\bar{d}_{ij} = 2$, $\forall (i,j) \in \mathcal{E}$, we ran 100 randomized ICs $z(0)$ and $\theta(0)$ and estimated the stability margin k_r via the bisection method. The range of these estimates and their maximum $k_r^*(n)$ for each n are shown in Figure 4.

As shown in the simulation results, one requires large gain ratios k_r to prevent the formation system (6) from diverging even when n is relatively small (e.g., for $n = 6$, we have $k_r^*(6) \approx 100$). Additionally, the monotonically increasing fit for $k_r^*(n)$ also suggests that the approach has poor scalability. In fact, the following proposition shows that system (6) cannot be globally convergent for *any* bounded k_r.

Proposition 1: Let a be an unbounded interaction law. Then, for any gain ratio k_r and network size n, there exists a rigid graph G, a target formation, and an initial condition $(\boldsymbol{z}(0), \boldsymbol{\theta}(0))$ such that the formation diverges to infinity.

Proof: For the case $n = 2$, let $\bar{d}_{12}$ be the target distance, let $d > \bar{d}_{12}$ be given, and take the symmetric ICs

$$\begin{bmatrix} x_i(0) & y_i(0) & \theta_i(0) \end{bmatrix} = \frac{(-1)^i}{2}\begin{bmatrix} d & 0 & \pi \end{bmatrix}. \tag{7}$$

From the symmetry of the ICs, the center of the formation is fixed at the origin $\forall t \geq 0$. At $t = 0$, $v = \|F_i\|$ is the tangential velocity along the circle and $\dot{\theta} = \dot{\tilde{\theta}}$ is the angular rotation rate. The sufficient condition $v > \dot{\theta} r$ for the agents to move radially outward at $t = 0$ is then

$$k_r < 4|a_{12}(d)|/\pi. \tag{8}$$

Since a_{12} is positive, monotonically increasing, and unbounded for $d > \bar{d}_{12}$, this inequality can be satisfied by sufficiently large d for any $k_r > 0$. Let such d be given which also satisfies $a_{12}(d) > 1$. We then have that $\dot{d}_{12}(0) > 0$ and $\frac{d}{dt}|\tilde{\theta}_i|_{t=0} > 0$. Moreover, $\dot{d}_{12}$ cannot be negative as long as $\tilde{\theta}_i \geq 0$. To achieve convergence, it follows by symmetry

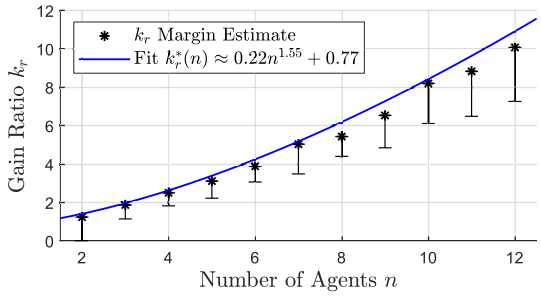

Fig. 5. Numerical approximation of the stability boundary $k_r^*(n)$ for the unbounded interaction law a. Experimental design is identical to Figure 4.

that the system would necessarily have to pass through a similar configuration (i.e., $|\tilde{\theta}_i| = \pi/2$) with $d_{12}(t) > d$. However, since (8) would also hold for any such $d_{12}(t) > d$, the system cannot converge to the target formation. Moreover, since $\|\boldsymbol{F}_i\|$ grows faster than d_{12} for any $a_{12}(d_{12}) > 1$, this initial condition and network topology will also diverge.

For $n > 2$, we construct a similar circular deployment using a spoke graph. Let $n-1$ of the agents be spaced equally around a circle with angular spacing $\phi = 2\pi/(n-1)$ and chord distance d between adjacent agents. Placing agent n at the origin with arbitrary orientation, the ICs for the remaining $n-1$ agents are given by

$$z_i(0) = r\begin{bmatrix}\cos((i-1)\phi)\\ \sin((i-1)\phi)\end{bmatrix}, \quad r = \frac{d}{2\sin(\frac{\phi}{2})},$$
$$\theta_i(0) = (i-1)\phi + (\pi/2). \tag{9}$$

We specify the target distance $\bar{d}$ between adjacent agents on the circle and the radial distances $\bar{r}$ to the center agent following the definition in (9). Noting that this deployment is symmetrically constrained in the same way as (7), the sufficient condition for outward radial motion is

$$k_r < 4(3 - 2\cos(\phi))|a_{ij}(d)|/\pi,$$

which can also be satisfied for all $(i,j) \in \mathcal{E}$ and any $k_r > 0$ by sufficiently large d for any $n > 2$. ■

B. Bounded Interaction Laws

Noting from Prop. 1 that an unbounded interaction law can cause the system to diverge, we now turn our attention to the case when the interaction law is bounded: i.e., $\|a_{ij}\|_\infty < \infty$, which ensures that the inter-agent forces F_i are globally Lipschitz. To investigate the stability of this case, we perform simulations similar to those in the previous subsection, with $a_{ij}(d_{ij}) = \frac{2}{\pi}\tan^{-1}(d_{ij} - \bar{d}_{ij})$. Comparing the results shown in Figure 5 with those from the unbounded case, we first note that the stabilizing $k_r^*(n)$ are much smaller. However, $k_r^*(n)$ is still increasing with n, indicating that the system is poorly-scalable. Based on these observations, we have the following conjecture:

Conjecture 1: For each n, there exists a minimum value $\bar{k}(n)$ such that, if the gain ratio $k_r > \bar{k}(n)$, then any system (6) of size n with finite $\|a_{ij}\|_\infty$ is almost globally convergent. However, $\bar{k}_r(n)$ is unbounded as $n \to \infty$.

Summarizing, we have the following stability issues for system (6) with bounded or unbounded interaction laws:

1) When the interaction laws are unbounded, the system is divergent for some ICs (Prop. 1). Our simulations also suggest that this set of divergent ICs is in fact open, as points in the neighborhood of the known divergent manifold also exhibit divergent behavior.
2) For both cases, simulations indicate that the gain ratio $k_r^*(n)$ grows with the network size n. Moreover, fit projections show that $k_r^*(n)$ is unbounded as $n \to \infty$.
3) For solutions that remain bounded, we cannot guarantee their convergence to static formations; indeed, there are cases where the system presents limit cycles. Even if solutions converge, there is no guarantee that they will converge to the set of local minima $\mathcal{A}_1$ of Φ.

C. Solution With Bump Functions

To resolve the stability issues presented above, we now propose a simple modification that, for any interaction law, ensures the same asymptotic behaviors of the nominal formation dynamics (2). To motivate this solution, recall the potential function $\Phi(z(t))$ defined for the nominal gradient dynamics given in (3). Considering the unicycle system (6), the dynamics of $\Phi(z(t))$ are then given by $\dot{\Phi}(z) = -\sum_{i=1}^n \cos(\tilde{\theta}_i)\|\boldsymbol{F}_i\|_2$. Note that if the agent orientation errors remain small ($\max_i|\tilde{\theta}_i(t)| \le \pi/2$) for all $t \ge 0$, then $\dot{\Phi}(z(t)) \le 0$ and the system will converge to some local minimum of Φ from almost all ICs. In contrast, a large error can cause the system to diverge as shown in Prop. 1. To address this issue, we augment the velocity dynamics of (6) with a plateaued, C^∞ bump function $\rho(\tilde{\theta}_i)$ of the form:

$$\rho(x) = \begin{cases} 1 & \text{if } |x| \le c_1 \\ \exp\left(1 - \frac{1}{1-\left(\frac{|x|-c_1}{c_2-c_1}\right)^2}\right) & \text{if } |x| \in (c_1, c_2) \\ 0 & \text{if } |x| \ge c_2, \end{cases} \tag{10}$$

where $c_1 = \pi/4$ and $c_2 = \pi/2$ are selected for this application. We then modify the control law as follows:

$$u_{v,i} = \rho(\tilde{\theta}_i)\|\boldsymbol{F}_i\|_2, \qquad u_{\tau,i} = -k_\theta\tilde{\theta}_i,$$

so that the resulting system dynamics are

$$\dot{\boldsymbol{z}}_i = \rho(\tilde{\theta}_i)\boldsymbol{R}(\tilde{\theta}_i)\boldsymbol{F}_i, \qquad \dot{\theta}_i = -k_\theta\tilde{\theta}_i, \tag{11}$$

By design, this bump function disables forward motion when an agent is poorly oriented ($|\tilde{\theta}_i(t)| \ge \pi/2$), thus nullifying the divergent behaviors discussed previously.

We will now state the convergence result for the modified system (11). Recall that the set $\mathcal{A}$ contains the *critical formations* (stable and unstable equilibria) of Φ, while $\mathcal{A}_1 \subseteq \mathcal{A}$ contains the local minima (stable equilibria) of Φ. Note that, if $z(t_0)$ belongs to $\mathcal{A}$ at certain time t_0, then $\dot{z}(t_0) \equiv 0$ and, hence, $z(t) \equiv z(t_0)$ for all $t \ge t_0$ regardless of the value of $\boldsymbol{\theta}(t)$. Finally, recall that for the nominal gradient dynamics (2), the formation system will converge to a local minimum in $\mathcal{A}_1$ from almost all ICs [18]. We will now establish the same stability guarantee for (11).

Theorem 1: Let Φ be the function defined in (3), let $\mathcal{A}$ and $\mathcal{A}_1$ be the set of critical formations and the set of local minima of Φ respectively, and let the bump function ρ be defined in (10). Then, Φ is a Lyapunov function for (11). Specifically, for any $(z(t), \boldsymbol{\theta}(t))$, we have that $\dot{\Phi}(z(t)) \leq 0$. Moreover, $\dot{\Phi}(z(t)) \equiv 0$ if and only if $z(t) \in \mathcal{A}$. As such, system (11) renders the set $\mathcal{A}_1$ almost globally stable.

Proof: We first obtain by computation that

$$\dot{\Phi} = \sum_{i=1}^{n} \dot{\Phi}_i, \qquad \dot{\Phi}_i = -\rho(\tilde{\theta}_i)\cos(\tilde{\theta}_i)\|\boldsymbol{F}_i\|_2.$$

It should be clear by the choice of ρ that $\dot{\Phi}_i \leq 0$ for all $i = 1, \ldots, n$ and, hence, $\dot{\Phi}(z(t)) \leq 0$. It now remains to show that if $\dot{\Phi}(z(t)) \equiv 0$, then $z(t) \in \mathcal{A}$.

We proceed by contradiction: assume that there exists a $z(t) \notin \mathcal{A}$ such that $\dot{\Phi}(z(t)) \equiv 0$. Since $\dot{\Phi}_i \leq 0$ by construction, this holds only if every $\dot{\Phi}_i \equiv 0$. Considering now a particular i and noting that $\cos(\tilde{\theta}_i) = 0 \Rightarrow \rho(\tilde{\theta}_i) = 0$, we have that $\dot{\Phi}_i \equiv 0$ only if $\rho(\tilde{\theta}_i)\|\boldsymbol{F}_i\| \equiv 0$. Since this product governs agent i's forward velocity, we then necessarily have that every agent remains stationary (in x, y). Thus, we have $\dot{d}_{ij} \equiv 0$ for all $(i, j) \in \mathcal{E}$ so that the system remains in critical formations. Additionally, each $\|\boldsymbol{F}_i\|$ also remains constant (as $\|\boldsymbol{F}_i\|$ is *only* a function of d_{ij}).

Consider now the bipartition of the agent index set:

$$\mathcal{I}^- := \left\{ i \mid |\tilde{\theta}_i(t)| < \frac{\pi}{2} \right\} \text{ and } \mathcal{I}^+ := \left\{ i \mid |\tilde{\theta}_i(t)| \geq \frac{\pi}{2} \right\}.$$

For each $i \in \mathcal{I}^-$, we must have $\|\boldsymbol{F}_i\| = 0$ so as to satisfy the assumption $\dot{\Phi}(z(t)) \equiv 0$. However, since $z(t) \notin \mathcal{A}$, there exists at least one $j \in \mathcal{I}^+$ such that $\|\boldsymbol{F}_j\| \neq 0$. Recall that

$$\bar{\theta}_j = \text{atan2}(\boldsymbol{F}_j), \quad \text{and} \quad \dot{\theta}_j(t) = -k_\theta\big(\theta_j(t) - \bar{\theta}_j(t)\big),$$

so that $\bar{\theta}_j(t)$ must also remain constant. As a result, the dynamics for $\tilde{\theta}_j(t)$ must obey the linear differential equation $\dot{\tilde{\theta}}_j(t) = -k_\theta \tilde{\theta}_j(t)$, so that $|\tilde{\theta}_j(t)|$ will be less than $\pi/2$ after some finite time t^*. Choosing t^* such that $\max_{j \in \mathcal{I}^+} |\tilde{\theta}_j(t^*)| = \pi/2$, we then have by continuity that there exists $\epsilon > 0, \delta > 0$ such that $\|\boldsymbol{F}_j(t^* + \epsilon)\| > 0$ and $|\tilde{\theta}_j(t^* + \epsilon)| < \pi/2 - \delta$. It then follows that

$$\dot{\Phi}(z(t^* + \epsilon)) \leq \dot{\Phi}_j(z(t^* + \epsilon)) < -\cos\left(\frac{\pi}{2} - \delta\right)\|\boldsymbol{F}_j\| < 0,$$

which contradicts our assumption that $\dot{\Phi}(z(t)) \equiv 0$. ■

By Theorem 1, the new system (11) is almost globally convergent to the set $\mathcal{A}_1$ (barring the finite unstable ICs in $\mathcal{A} \backslash \mathcal{A}_1$). Thus, Theorem 1 shows that (11) have the *same* stability guarantees as the nominal gradient dynamics (2). Notably, if the underlying graph G is a triangulated Laman graph, then $\mathcal{A}_1$ contains *only* the target formations [18], so that (11) converges to a target formation from almost all ICs.

IV. Convergence Time and Energy Consumption

Having established the almost global convergence properties of dynamics (11) (see Figure 6 for example simulations), we now examine the performance impact of the bump function on the bounded interaction law. We also compare this

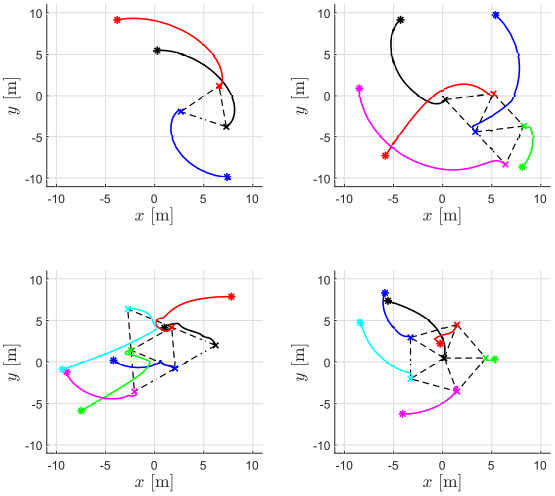

Fig. 6. Example simulations of various triangulated Laman graph formations with $d_{ij} = 5$ m. Results (a-c) use Henneberg graphs with $n = 3, 5$, and 6 agents, and (d) uses a spoke graph with $n = 6$.

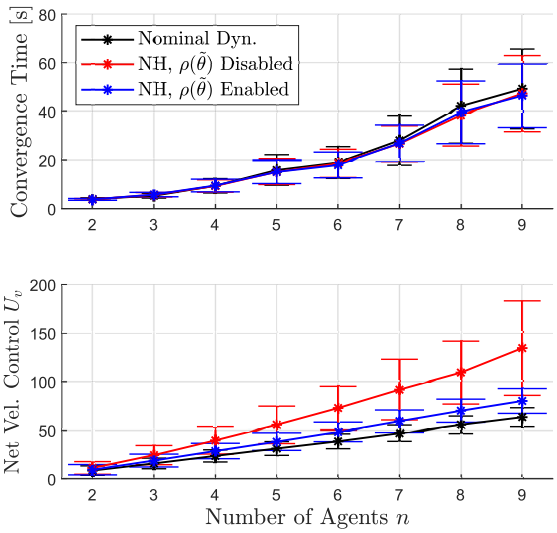

Fig. 7. Comparative performance of the nominal and bounded nonholonomic unicycle dynamics with and without the bump function. Error bars show a $\pm\sigma$ range for a Gaussian fit of each metric for each n.

system's performance against that of the nominal dynamics (2). System performance is evaluated for Henneberg graph constructions with $\bar{d}_{ij} = 2$ m using the following metrics: the formation convergence time T and total velocity control effort U_v. Following the result of Theorem 1, formation convergence is measured using the normalized potential function gradient $C(z) = k_v^{-1}\|\dot{\Phi}\|$ where $C(z(t)) < 10^{-3}$ for all $t \geq T$ indicates convergence at time T. The total normalized control effort U_v is then computed as

$$U_v = k_v^{-1} \sum_i \int_0^T \|F_i(t)\| dt.$$

These metrics were determined numerically for each network size n via a Gaussian fit of the simulation results for 500 randomized ICs. Following the results in Figure 5, we select a sufficiently large $k_r = 8$ to ensure the convergence of the bounded law for the range $n = 2$ to $n = 9$. Note that, for

$n > 10$, convergence would no longer be guaranteed in the absence of a bump function.

Examining the mean convergence times shown in panel (a) of Figure 7, we first note that there is no significant statistical difference between the convergence times of any of the methods with respect to the nominal dynamics. In contrast, the results in panel (b) display a significant difference in the applied velocity control for each method. Naturally, the nominal dynamics are the most efficient, as the control actuation $\|\boldsymbol{F}_i\|$ is always ideally directed. The bounded unicycle construction then exceeds this nominal cost by 78% on average and the inclusion of the bump function reduces this excess to 22%. From these results and Theorem 1, we conclude that the bump function augmentation improves the system in both stability and performance.

V. Conclusion

We investigated stability properties of a formation of unicycles by adapting a gradient control law. It was found that a direct inner-outer loop cascade formulation of the unicycle controller introduces stability issues dependent upon the time-scale separation of the inner and outer loops by means of the gain ratio k_r. Sufficiently large stabilizing k_r were found to increase without bound if the formation size n grows, indicating issues in scalability. It was also found that no single k_r could guarantee almost global convergence to the target formation for arbitrary formation size. In response, we introduced bump functions to ensure almost global convergence to stable critical formations of any size. The performance of this solution was validated numerically and found to have a convergence rate similar to the nominal gradient dynamics and less energy consumption compared to the direct inner-outer loop approach.

References

[1] J. Qin, Q. Ma, Y. Shi, and L. Wang, "Recent advances in consensus of multi-agent systems: A brief survey," *IEEE Trans. Ind. Electron.*, vol. 64, no. 6, pp. 4972–4983, Jun. 2017.

[2] H. Goldstein, C. P. Poole, Jr., and J. L. Safko, *Classical Mechanics (3rd Edition)*. Upper Saddle River, NJ, USA: Pearson, 2002.

[3] M. Hua, T. Hamel, P. Morin, and C. Samson, "Introduction to feedback control of underactuated VTOLvehicles: A review of basic control design ideas and principles," *IEEE Control Syst. Mag.*, vol. 33, no. 1, pp. 61–75, Feb. 2013.

[4] S. Chung, A. A. Paranjape, P. Dames, S. Shen, and V. Kumar, "A survey on aerial swarm robotics," *IEEE Trans. Robot.*, vol. 34, no. 4, pp. 837–855, Aug. 2018.

[5] K.-K. Oh, M.-C. Park, and H.-S. Ahn, "A survey of multi-agent formation control," *Automatica*, vol. 53, pp. 424–440, Mar. 2015.

[6] M. Maghenem, A. Bautista, E. Nuno, A. Loria, and E. Panteley, "Consensus of multi-agent systems with nonholonomic restrictions via Lyapunov's direct method," *IEEE Control Sys. Lett.*, vol. 3, no. 2, pp. 344–349, Apr. 2019.

[7] A. Sadowska, D. Kostic, N. V. D. Wouw, H. Huijberts, and H. Nijmeijer, "Distributed formation control of unicycle robots," in *Proc. Int. Conf. Robot. Autom.*, Saint Paul, MN, USA, 2012, pp. 1564–1569.

[8] T. Liu and Z.-P. Jiang, "Distributed formation control of nonholonomic mobile robots without global position measurements," *Automatica*, vol. 49, no. 2, pp. 592–600, 2013.

[9] X. Cai and M. D. Queiroz, "Adaptive rigidity-based formation control for multirobotic vehicles with dynamics," *IEEE Trans. Control Syst. Technol.*, vol. 23, no. 1, pp. 389–396, Jan. 2015.

[10] E. K. Xidias and P. N. Azariadis, "Computing collision-free motions for a team of robots using formation and non-holonomic constraints," *Robot. Auton. Syst.*, vol. 82, pp. 15–23, Aug. 2016.

[11] D. Panagou, D. M. Stipanović, and P. G. Voulgaris, "Distributed coordination control for multi-robot networks using Lyapunov-like barrier functions," *IEEE Trans. Autom. Control*, vol. 61, no. 3, pp. 617–632, Mar. 2016.

[12] H. Gutierrez, A. Morales, and H. Nijmeijer, "Synchronization control for a swarm of unicycle robots: Analysis of different controller topologies," *Asian J. Control*, vol. 19, no. 5, pp. 1822–1833, 2017.

[13] S. Mastellone, D. M. Stipanović, C. R. Graunke, K. A. Intlekofer, and M. W. Spong, "Formation control and collision avoidance for multi-agent non-holonomic systems: Theory and experiments," *Int. J. Robot. Res.*, vol. 27, no. 1, pp. 107–126, 2008.

[14] S. Zhao and D. Zelazo, "Bearing rigidity theory and its applications for control and estimation of network systems: Life beyond distance rigidity," *IEEE Control Syst. Mag.*, vol. 39, no. 2, pp. 66–83, Apr. 2019.

[15] G. Jing, G. Zhang, H. W. J. Lee, and L. Wang, "Angle-based shape determination theory of planar graphs with application to formation stabilization," *Automatica*, vol. 105, pp. 117–129, Jul. 2019.

[16] L. Krick, M. E. Broucke, and B. A. Francis, "Stabilisation of infinitesimally rigid formations of multi-robot networks," *Int. J. Control*, vol. 82, no. 3, pp. 423–439, 2009.

[17] S. Mou, M.-A. Belabbas, A. S. Morse, Z. Sun, and B. D. O. Anderson, "Undirected rigid formations are problematic," *IEEE Trans. Autom. Control*, vol. 61, no. 10, pp. 2821–2836, Oct. 2015.

[18] X. Chen, M.-A. Belabbas, and T. Başar, "Global stabilization of triangulated formations," *SIAM J. Control Optim.*, vol. 55, no. 1, pp. 172–199, 2017.

[19] U. Helmke and B. D. O. Anderson, "Equivariant Morse theory and formation control," in *Proc. 51st Annu. Allerton Conf. Commun. Control Comput.*, Monticello, IL, USA, 2013, pp. 1576–1583.

[20] X. Chen, M.-A. Belabbas, and T. Başar, "Controlling and stabilizing a rigid formation using a few agents," *SIAM J. Control Optim.*, vol. 57, no. 1, pp. 104–128, 2019.

[21] M. A. Belabbas, "On global stability of planar formations," *IEEE Trans. Autom. Control*, vol. 58, no. 8, pp. 2148–2153, Aug. 2013.

[22] R. Naldi, M. Furci, R. G. Sanfelice, and L. Marconi, "Robust global trajectory tracking for underactuated VTOL aerial vehicles using inner-outer loop control paradigms," *IEEE Trans. Autom. Control*, vol. 62, no. 1, pp. 97–112, Jan. 2017.